J Mater Sci (2008) 43:7210–7218
DOI 10.1007/s10853-008-2958-6

Wet fiber shear flexibility and its contribution to the overall transverse deformation of fibers

Dongbo Yan · Kecheng Li

Received: 16 March 2008 / Accepted: 18 August 2008 / Published online: 27 September 2008

Abstract A new method has been developed for measuring not only bending but also shear flexibility of pulp fibers by using confocal laser scanning microscopy. Based on the Steadman and Luner method, a two-stage wet pressing process was used which enabled both bending and shear flexibility and both bending and shear modulii of fibers to be determined with a single test. Three types of fibers, i.e., bleached spruce Kraft Pulp (BKP), aspen bleached chemi-themomechanical pulp (BCTMP), and aspen themomechanical pulp (CTMP), were tested. Results show that the longitudinal elastic modulii of the fibers are in a range of 3–37 GPa, and the transverse shear modulii of them are in a range of 27–103 MPa. It was also found that the shear contribution to the overall fiber deformation ranged from 60% to 90% for the fibers measured. This substantiates the concept of shear contribution to measured fiber flexibility as proposed by Waterhouse and Page.

Introduction

Wet fiber conformability refers to how easy individual fibers can conform to each other to form a well-bonded paper sheet structure in the papermaking process. Flexible fibers bend easily under transverse stresses by the capillary force of water during papermaking processes. Therefore, several methods have been developed for measuring wet fiber flexibility in order to evaluate the conformability of wet fibers during paper consolidation process [1–5].

D. Yan (✉) · K. Li
Department of Chemical Engineering and Limerick Pulp and Paper Research and Education Centre, University of New Brunswick, Fredericton, NB, Canada E3B 6C2
e-mail: g216d@unb.ca

Recently, Waterhouse and Page [6] found that shear deformation could contribute significantly to the overall deformation of the fibers as analyzed in all the existing fiber flexibility measurement methods. It is incorrect to neglect the shear contribution in the bending flexibility measurement. According to their calculation using an E/G ratio of 2000, where E is the longitudinal elastic modulus and G is the transverse shear modulus of fiber, the contribution of shear to overall deflection varies from insignificant to overriding in different flexibility measurement methods, depending on the freespan length used in each method [6]. Therefore, they concluded that given the fiber span length is only about the order of a fiber width, the fiber deformation in real paper is almost entirely due to shear.

The methods reported include hydrodynamic or bending beam method, and conformability method. In hydrodynamic methods, fibers are bended either as a cantilever beam [2, 3] or a simply supported beam [4]. The bending force is applied by a water stream which is calculated with the hydrodynamic theory. In the conformability test [5, 7], wet fibers are pressed onto a thin wire and form arcs over it. The deformation of the fibers is measured by a microscope and is then related to the wet fiber flexibility. In all these methods, fiber flexibility is expressed as the bending flexibility, $F_B = 1/EI$, where fibers are treated as an ideal elastic beam that deforms only by bending.

In order to evaluate shear contribution to the overall fiber deformation, both elastic modulus E and the shear modulus G must be known. The E of a single fiber is usually measured from load-elongation curves that are obtained with micro-tensile tests [8–12]. The difficulties associated with those tests are the requirement of handling individual fibers and accurate measurement for the stress and strain on a small scale [13, 14]. Those drawbacks make this method impractical for engineering applications [15].

The shear modulus of wet fiber has been relatively rarely studied for papermaking fibers. Theoretically, G could be obtained by performing twisting test on a single fiber with a micro-torsion apparatus assuming that a fiber is a homogeneous, isotropic and elastic circular shaft or tube [16–19]. Since fibers are liable to twist rather than deform when subjected to torsion, those tests usually measure the torsion rigidity other than the shear modulus [17, 20]. Because of this, the shear modulus of wet pulp fibers is hard to be measured experimentally. It is usually estimated from the transverse modulus *E33* [6]. The *E33* can be measured with the micro-compression test [21–23] or the AFM indention test [24]. Similar to the measurement of longitudinal modulus, handling and measuring an individual fiber are required for measuring the *E33*. Because fibers are not totally collapsed, it is hard to isolate the deformation of fiber wall from the displacement caused by the collapse of lumen under transverse compressing. The reported *E33* for a same fiber type, i.e., spruce kraft pulp fibers, varies in a wide range from 4 MPa [25] to 560 MPa [23].

In our previous studies [26, 27], a new method was developed by using confocal laser scanning microscopy (CLSM) for fiber flexibility measurement. Using CLSM, the transverse section and the cross section of fibers can be observed directly. Therefore, not only the mode of fiber deformation, i.e., bending deformation or shear deformation, can be identified, but also the fiber cross section area and the moment of inertia can be measured. This provides opportunity for calculating the E and G with an appropriate procedure of fiber flexibility measurement. The objective of this investigation is to develop a method for measuring both fiber bending flexibility and shear flexibility. By analyzing the separated bending and shear flexibility, the nature of fiber deformation in real papermaking process can be better understood.

Theory

Fiber deformation model

Fibers deform differently with the forces and constraints they are subjected to Ebling [28] proposed a model to describe the fiber–fiber interactions during consolidation and dewatering in the real papermaking process, in which the fiber wall deformed under the drying-induced stress that is caused by the capillary forces. The transverse deflections are about the order of fiber thickness, and the spans are on the order of the fiber width. This type of deformation is supported by SEM Images of some paper samples [29, 30]. The model can be simplified as a fiber bending over others (Fig. 1). The forces that induce fiber transverse deformation, e.g., capillary force and mechanical pressure, are

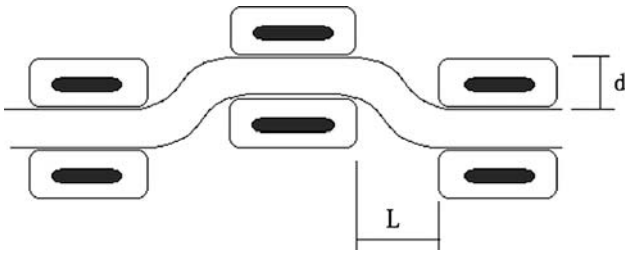

Fig. 1 Schematic illustration of the simplified geometry of fiber deformation in paper

represented by a uniformly distributed load q (Fig. 2). The total deflection Δ in transverse direction y is restricted by the fiber thickness d. The span length caused by the load q is L. The Δ of fiber end is assumed to consist of two portions—bending deflection (δ_b) and shear deflection (δ_s).

$$\Delta = \delta_b + \delta_s \tag{1}$$

If the fiber is treated as a statically indeterminate beam that is subjected to a uniform distributed transverse load, the bending deflection δ_b can be calculated by following the Steadman procedure [5], as shown in Eq. 2.

$$\delta_b = \frac{qL^4}{72EI} \tag{2}$$

The shear deflection δ_s at the free end can be calculated by assuming the fiber as a cantilever beam. It also consists of two portions, δ_{su}, which is induced by the distributed load $q = -w$, and δ_{sc}, which is induced by the shear forces between R_a and R_b. The δ_{su} is the shear deflection portion of the cantilever beam due to distributed load w, which can be calculated with the unit-load method based on the principle of virtual work [30].

$$\delta_{su} = \frac{2f_s}{GA}\int_{x=0}^{L} w(L-x)dx = \frac{wf_s}{GA}[xL - \frac{x^2}{2}]_0^L = \frac{wf_s}{GA}L^2 \tag{3}$$

The δ_{sc} is the shear deflection of a cantilever beam due to concentrated force at the free end. The shear force P is the differential of R_a and R_b [5].

$$P = R_a - R_b = \frac{wL}{4} - \frac{6EI\delta_b}{L^3} = \frac{wL}{6} \tag{4}$$

$$\delta_{sc} = \frac{Pf_s}{GA}L = \frac{1}{3}\frac{wf_s}{GA}L^2 \tag{5}$$

where G is fiber shear modulus and A is the cross-section area. f_s is the shape factor of fiber cross section [30]. For a thin-wall cylindrical uncollapsed fiber, $f_s = 2$, and for a totally collapsed fiber, $f_s = 6/5$. In this paper, the shear flexibility, $F_S = f_s/GA$, which is the reciprocal of the shear rigidity, will be used [31].

The total deflection in fiber thickness direction can be expressed as

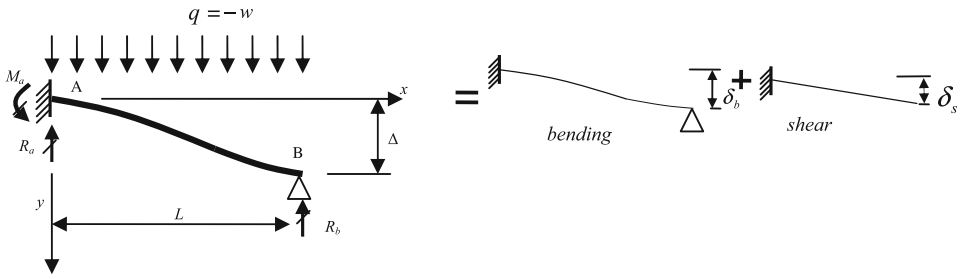

Fig. 2 Beam deformation under transverse forces and the contribution of bending and shear deformation

$$\Delta = \frac{w}{72EI}L^4 + \frac{4}{3}\frac{f_s w}{GA}L^2. \tag{6}$$

In order to evaluate the contribution of shear to overall deformation, the ratio of shear to bending deflection is used

$$\frac{\delta_s}{\delta_b} = \left(\frac{4}{3}\frac{f_s w L^2}{GA}\right) / \left(\frac{wL^4}{72EI}\right) = \frac{96}{L^2}\frac{F_S}{F_B}. \tag{7}$$

It can be seen that the shear contribution is determined by the F_S/F_B ratio and the span length, where F_B is the bending flexibility.

Methodology

According to Eq. 6, the total deflection is determined by the span length for given fiber geometry, (A, I, f_s) and material properties (E, G). If the Steadman method is used, the deflection Δ can be fixed as the diameter of the support wire (d) and Eq. 6 can be written as

$$\frac{d}{w} = \frac{L^4}{72EI} + \frac{4}{3}\frac{f_s}{GA}L^2. \tag{8}$$

Using CLSM, the freespan length (L) can be measured directly and I and A can be calculated with the fiber cross-section dimension measured by CLSM. Therefore, there are only two unknowns, E and G, in the equation. If two loads, w_1 and w_2, are applied to the same fiber spanning over a support wire, two sets of knowns, (L_1, A_1, I_1) and (L_2, A_2, I_2) can be obtained, and hence the two unknowns (E, G) can be resolved. Following the reasoning line in this study, a double pressing procedure was developed. Fibers were first pressed at load w_1 and the freespan L_1 was measured. Fibers were then rewetted and pressed at load w_2, ($w_2 > w_1$), by which the freespan was decreased to L_2. If the cross-section shape does not change during wet pressing, A and I are constant. The shear and bending flexibility can be solved,

$$F_S = \frac{f_s}{GA} = \frac{3d}{4}\frac{1}{w_1 w_2}\frac{w_1 L_1^4 - w_2 L_2^4}{L_1^4 L_2^2 - L_1^2 L_2^4} \tag{9}$$

$$F_B = \frac{1}{EI} = 72d\frac{1}{w_1 w_2}\frac{w_1 L_1^2 - w_2 L_2^2}{L_1^4 L_2^2 - L_1^2 L_2^4}. \tag{10}$$

Since some fibers, especially mechanical fibers, usually only collapse partially, the cross-section shapes change during the double wet pressing process. Therefore, the cross-section dimension needs to be measured for the same fiber after each pressing. The E and G can be solved by Eq. 9 with two sets of data, and the shear and bending flexibility can be calculated from E, G and fiber cross-section parameters accordingly.

$$\frac{1}{E} = 72d\frac{I_1 I_2}{w_1 w_2}\frac{w_1 A_1 L_1^2 - w_2 A_2 L_2^2}{A_1 I_2 L_1^2 L_2^4 + A_2 I_1 L_1^4 L_2^2} \tag{11}$$

$$\frac{1}{G} = \frac{3d}{4}\frac{1}{f_s}\frac{A_1 A_2}{w_1 w_2}\frac{w_1 I_1 L_1^4 - w_2 I_2 L_2^4}{A_1 I_2 L_1^2 L_2^4 + A_2 I_1 L_1^4 L_2^2} \tag{12}$$

Experimental

Sample preparation

Aspen chemi-thermomechanical pulp (CTMP), bleached aspen chemi-thermomechanical pulp (BCTMP), and bleached spruce kraft pulp (BKP) from Canadian paper mills were used. Pulp fibers (0.3 g o.d) were stained in 20 mL 0.1% Safaranin-O for 24 h at room temperature to enhance the fluorescence intensity, and then diluted to 0.03% consistency with distilled water and drained onto a piece of filter paper (Fisher brand Q8) by a TAPPI standard handsheet former. The suspension was swirled before draining to orient pulp fibers in parallel on the filter paper.

Single quartz fibers (CPI international PN: 511-735) with a nominal diameter of 10 μm were manually laid in the middle of a microscope glass slide (Fisher brand pre-cleaned microscope slide), with two ends fixed on the glass slide by the proxy glue.

The pulp fibers were then transferred from the filter paper onto the prepared microscope slides by placing and gently tapping the filter paper onto the slides. The filter paper was replaced with a Millipore filter (Millipore, GPWP04700), and covered with 2 dry blotting papers and pressed by standard handsheet press at 340 kPa for 3 min. Seven additional glass slides were pressed along with sample slides to distribute the press load evenly. The actual load applied to the sample was calculated according to the total area of the glass slides. The slides were air dried and kept under TAPPI standard conditions before CLSM imaging. Once all fibers have been imaged with CLSM, the

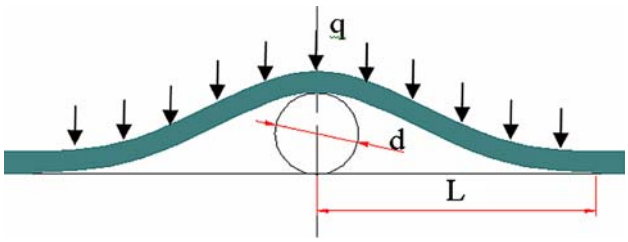

Fig. 3 Beam deflection geometry in the Steadman and Luner method [5]

specimens were covered with a Millipore filter and rewetted with water applied by a wool roller. They were covered with 2 dry blotting papers and pressed at 460 kPa for 3 min, followed by another CLSM imaging (Fig. 3).

CLSM imaging

Image scanning was carried out with a Leica TCS-SP2 confocal laser scanning system. Images were obtained with a dry objective lens (HC FLOUTAR 50 × 0.8). Excitation wavelength of 514 nm from an *Ar* laser is used. The pinhole size is set at the optimum value by the Leica Confocal Control software. The emission light from 525 to 760 nm was collected by detector (PMT). The gain and offset of PMT were automatically adjusted for each fiber by software to ensure a constant image quality. CLSM is operated at *XZ* or *YZ* scanning mode to obtain transverse and cross-sectional image for dimension measurement. Scanning step size in *Z* direction is 0.12 μm. The lateral resolution is 0.29 μm/pixel in transverse CLSM images. 4× digital zoom was used when imaging fiber cross section. The nominal resolution is 73 nm/pixel. Typical original CLSM images are shown in Figs. 4 and 5. Only well-defined fibers with smooth and symmetric span curves were measured.

Image analysis

CLSM transverse images were converted to binarized images. The threshold was auto-determined by ImageJ, which is an optimized value between the average of background and the objects [32, 33]. Freespan length and deflection height were measured at the neutral bending plane of fiber transverse profile, which was defined as the symmetric center in fiber thickness along the fiber length according to our previous study [26], as shown in Fig. 6.

Fiber width, thickness, and cross-section area were measured from the binarized cross-sectional CLSM images, as shown in Fig. 5. Since the cross-section shape of most fibers is nearly rectangular, Eq. 13 is used for calculating the moment of inertia *I*. The area of fiber cross section is measured automatically with the software by summing up the area of all the pixels

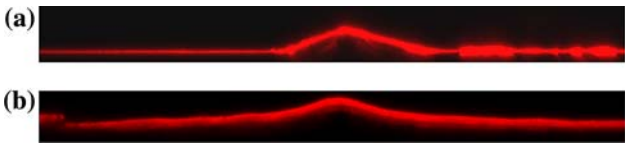

Fig. 4 Typical CLSM image of the transverse optical slice of pulp fibers that wet pressed at 340 kPa on a glass rod. (**a**) Spruce BKP, wet pressed at 340 kPa. Shear contribution 91%; (**b**) Aspen BCTMP, wet pressed at 340 kPa. Shear contribution 68%. Image size 300 × 26.3 μm

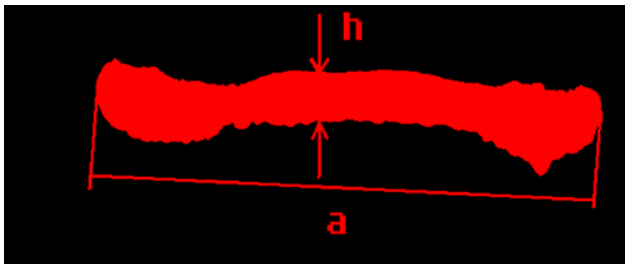

Fig. 5 Binarized image of the cross section of an aspen BCTMP fiber that wet pressed at 340 kPa. Measured fiber width 18.6 μm, height 4.13 μm and the cross-section area 76.78 μm^2

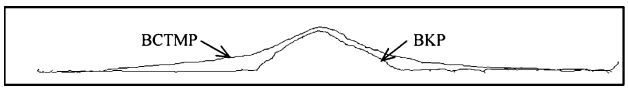

Fig. 6 The subtracted "neutral bending planes" from Fig. 4. The freespan length measured is 117.38 μm (left) and 105.76 μm (right) for aspen BCTMP, and 30.75 μm (left) and 42.05 μm (right) for spruce BKP

$$I = \frac{ah^3}{12}. \tag{13}$$

Since the thickness of fibers is usually not a constant, it was measured manually and the average values were used for the calculation. All image processing were performed with an open source image processing software—ImageJ [31].

Results and discussion

Elastic and shear modulii of the fiber wall

With a two-stage pressing process, two sets of measurements were obtained including the freespan length (L_1, L_2), the fiber cross-section area (A_1, A_2) and the fiber moment of inertia (I_1, I_2), as shown in Table 1. The shear modulus (G) and elastic modulus (E) were then calculated according to Eqs. 12 and 13, which are listed in Table 1. It can be seen that for BKP fibers, the difference in I and A change after each wet pressing is minimal. This is because the BKP fibers collapse completely under pressure load, so the

Table 1 Test results obtained from a two-stage wet-pressing method

Pulp	L_1 (μm)	L_2 (μm)	I_1 ($\times 10^{22}$, m^4)	I_2 ($\times 10^{10}$, m^2)	A_1 ($\times 10^{10}$, m^2)	A_2 ($\times 10^{10}$, m^2)	G (MPa)	E (GPa)	E/G ratio
BKP	91.69	36.959	0.99	0.95	1.06	1.06	27.57	3.14	114
BCTMP	109.51	53.029	2.01	1.62	1.06	1.05	79.61	18.86	237
CTMP	200.38	89.98	6.44	6.95	1.65	1.38	102.95	37.19	361

Note: (1) 15 fibers were measured for each sample and the median values are presented. (2) Wet pressing pressure for BKP: $P_1 = 220$ kPa, $P_2 = 340$ kPa; and for BCTMP and CTMP: $P_1 = 340$ kPa, $P_2 = 460$ kPa

geometry of the fiber cross section remains basically the same after each of the wet processing. For CTMP fibers, the difference in *I* and *A* after the first and the second wet pressing is apparent. This indicates that the first pressing stage further collapses the fiber lumen structure. The calculated shear and elastic modulii for all the three types of fibers are quite scattered as shown in Fig. 7. This is expected since each fiber of the same pulp can be different in terms of both their material structure and the chemical components. Even for the same fiber, different location on the fiber may give different results. Therefore, median values are reported and compared with that of other studies.

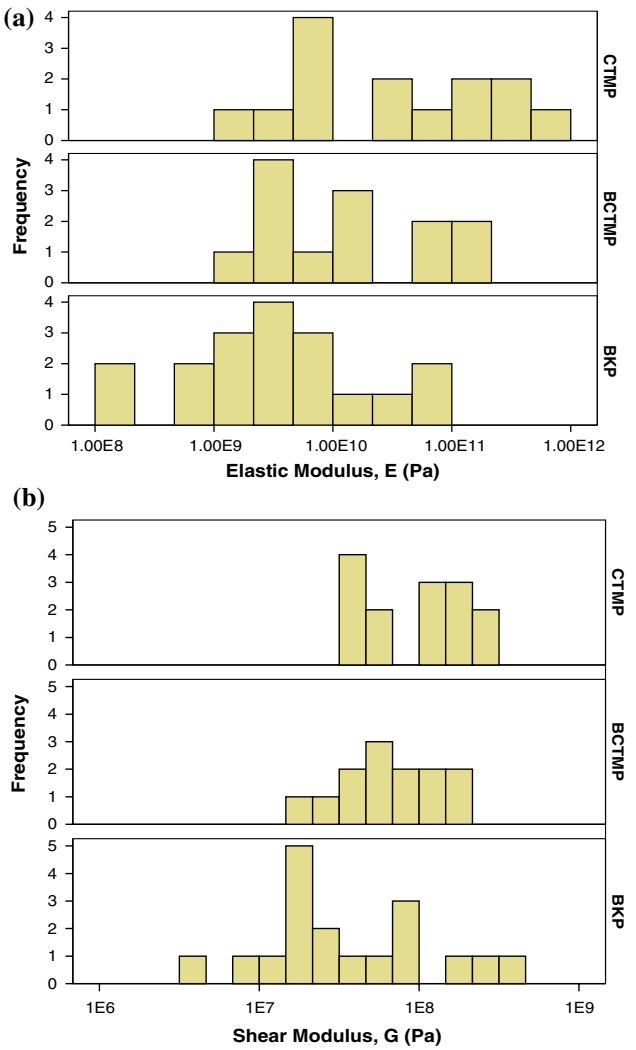

Fig. 7 Distribution of measured values *E* (**a**) and *G* (**b**) of three different types of pulp fibers

As shown in Table 1, the median value of elastic modulus of BKP fibers is 3.14 GPa. According to Ehrnrooth and Kolseth [12] the *E* of Norway spruce Asplund pulp and a Norway spruce pulp prepared by delignifying with sodium chlorite to 62.4% deligninfication level were 9.2 GPa and 4.3 GPa with axial tensile method, respectively. This agrees well with the results obtained in the present study. Compared with BKP, aspen mechanical fibers show much higher modulus. The *E* of the CTMP is 37.19 GPa. This may be due to the high lignin concentration in the fiber wall and on the fiber surface of CTMP [34], since lignin has relatively higher elastic modulus [35]. In contrast, the *E* of the BCTMP fibers is only 18.86 GPa, indicating that bleaching modifies the lignin structure or removes certain compounds from the fiber cell well.

According to Waterhouse [6], shear modulus can be estimated from the Poisson's ratio and transverse modulus *E33*, the shear modulus of pulp fibers is estimated to be 3/8 of the *E33* of pulp fibers. Quite a range of *E33* values has been reported in the literature. Higher *E33* values, 350–750 MPa, were reported by Hartler and Nyren [21, 36]. Lower values of *E33*, 6.5–9.3 MPa, were reported by Wild [37] with transverse Micro-compression method. Page [13] obtained a theoretical value to be about 8.8 GPa based on the cellulose-hemicellulose-lignin composite model. In the present study, the *G* values of spruce BKP, aspen BCTMP and CTMP is about 28 MPa, 80 MPa, and 103 MPa, respectively. Dunford and Wild [23] found that different transverse modulus might be obtained if measured at different transverse load for the transverse displacement including the lumen collapse and fiber wall compression. The apparent modulus obtained ranges from a few MPa to about 60 MPa with the increasing testing forces. With cyclic loading, the *E33* reached to about 130 MPa after 30 load cycles. The shear modulus corresponding to it is about 48 MPa. Since the fibers have been subjected to wet pressing twice at a higher pressure, higher transverse modulus is expected with the present method. In general, the *G* is of same order of magnitude as that estimated from transverse modulus by Dunford and Wild [23].

The shear modulus measured in the present study, 28–103 MPa, is much higher than the value (5 MPa) used by Waterhouse and Page [6] for comparing the shear contribution, but the E measured in this study is on the order of 10 GPa. Therefore, the E/G ratio obtained in the present experiment is from 100 to 300 in comparison with 2000 as used by Waterhouse and Page [6].

In order to validate the method developed, statistical analysis (Oneway ANOVA) was used to analyze the significance of the difference among the E and the G of the three types of fibers. The results show that the significance (Sig.) is 0.035 and 0.05 for E and G, respectively. With the Oneway ANOVA analysis, a Sig. <0.05 is considered significantly different. This means that the double pressing method developed is able to differentiate different types of pulp in terms of their E and G.

Shear and bending flexibility of fibers

With the elastic modulus and shear modulus calculated and the A and I of fibers measured, the bending flexibility and shear flexibility can be calculated directly according to Eqs. 11 and 12. Table 2 lists the calculated shear and bending flexibility after each stage after the wet pressing. To compare, the Steadman method was also used for calculating the flexibility, which is the flexibility calculated from the free span length and deflection height assuming a pure bending situation. It can be seen that both shear and bending flexibilities of bleached spruce kraft fibers are almost the same of each of the two pressing at different pressures. This can be explained by the almost unchanged A and I after each pressing as listed in Table 1. However, the difference of mechanical fibers is significant. In general, both shear and bending flexibility increased with the pressing pressure, due to the reduced cross-section area A and moment of inertia I.

The flexibility of unbleached spruce kraft fibers measured with hydrodynamic method is 3.66×10^{-11} N^{-1} m^{-2} by Tam Doo [4], and 1.81×10^{-11} N^{-1} m^{-2} by Kuhn [3]. Since the shear contribution in their method is very small [6], the results can be considered as a measure of the pure bending flexibility. In this study, the bending flexibility of bleached spruce kraft fibers obtained is 26.42×10^{-11} N^{-1} m^{-2}. It is much higher than that of unbleached fibers. However, if we calculate the bending flexibility by using the elastic modulus of BKP fiber, 4.3 GPa, measured by Ehrnrooth [12] and the moment of inertia, 0.99×10^{-22} m^4, as measured in the present experiment, the results will be 23.49×10^{-11} N^{-1} m^{-2}, which is almost the same as the result obtained for spruce BKP fibers. The flexibility obtained with the Steadman method is usually much higher than the bending flexibility, especially for the fibers after the second stage pressing,

Table 2 Fiber flexibility obtained with a two-stage wet pressing method

Pulp	Deflection ratio @ P_1, %	Deflection ratio @ P_2, %	Shear flexibility @ P_1, N^{-1}	Shear flexibility @ P_2, N^{-1}	Bending flexibility @ P_1, $\times 10^{-11}$ N^{-1} m^{-2}	Bending flexibility @ P_2, $\times 10^{-11}$ N^{-1} m^{-2}	Steadman flexibility @ P_1, $\times 10^{-11}$ N^{-1} m^{-2}	Steadman flexibility @ P_2, $\times 10^{-11}$ N^{-1} m^{-2}	Shear contribution @ P_1%, %	Shear contribution @ P_2, %
BKP*	13.09	32.47	407.63	407.79	26.42	27.53	27.60	335.48	63.79	91.24
BCTMP	10.96	22.63	183.8	177.76	7.30	8.00	21.10	131.66	66.84	88.35
CTMP	6.00	13.34	54.55	64.94	0.25	0.84	1.27	7.14	83.91	90.16

Note: (1) 15 fibers were measured for each sample and the median values are presented. (2) Wet pressing pressure for BKP: $P_1 = 220$ kPa, $P_2 = 340$ kPa; and for BCTMP and CTMP: $P_1 = 340$ kPa, $P_2 = 460$ kPa

since in the Steadman method, all the deflection is attributed to a pure bending.

Little has been found in the literature with regards to fiber shear flexibility, due to the difficulties in measuring the shear flexibility of fibers. However, the shear contribution to the overall fiber deformation is substantial as listed in Table 2. The contribution is from 64% to 84% for the three types of fibers after the first wet pressing. Pressing with higher pressure in the second pressing stage, the shear contribution is further increased to about 90% for all the three fibers. This result is in accordance with Waterhouse and Page's [6] analysis, that is, the shorter the span, the higher the shear contribution.

The measured shear flexibility for the three types of fibers is quite different, from as high as about 400 N^{-1} for the BKP fibers and as low as about 50 N^{-1} for the CTMP fibers. This is mainly attributed to the difference in their G value. The effect of the cross-section area is relatively small in this case.

The contribution of shear to the overall fiber deformation can also be directly observed from the shape of the deformed fibers with CLSM. As shown in Fig. 4, the shape of the BKP fiber span over a support wire is almost like two segments of straight lines, featuring a shear deformation. In contrast, the span of the aspen BCTMP fiber is most curved, exhibiting the feature of a bending deformation. The calculated shear contribution for the fibers shown in Fig. 4a is 91% and that of the fiber in Fig. 4b is 68%.

Evaluation of the shear contribution to fiber deformation in real paper

According to Waterhouse and Page [6], the span length is the predominant factor in determining the contribution of shear to the overall fiber deformation under transverse stresses. This can be seen from Eq. 7, in which the shear flexibility (F_S) and bending flexibility (F_B) are constants for a given fiber geometry, so the ratio of shear to bending deformation is inversely proportioned to the second power of the span length (L). A small L will result in a large shear to bending ratio. The relationship between L and shear contribution is illustrated in Fig. 8. It can be seen that when the span length is below 100 μm, the shear contribution ranges from 60 to 95% depending on E/G ratio, i.e., the type of fiber.

In a real paper structure, the span length is about the width of a fiber according to references [30, 38] In fact, with CLSM, the deformation of a fiber over another fiber can be directly observed. Figure 9 shows the intersection of two aspen BCTMP fibers. It can be seen that the span length of the overlaying fiber is about the same as the width of the underlying fiber, and the deflection height is determined by the thickness of the underlying fiber. This

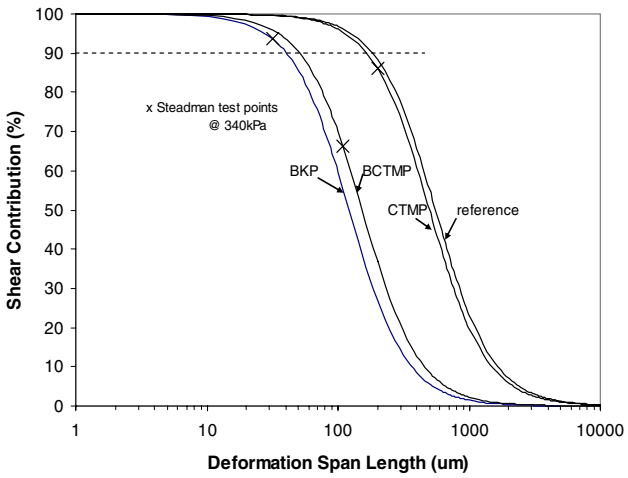

Fig. 8 Contribution of shear to the overall deformation versus the span length in the conformability test method. The reference line is calculated based on $E/G = 2000$ and $h = 4$ μm, according to Waterhouse and Page [6]

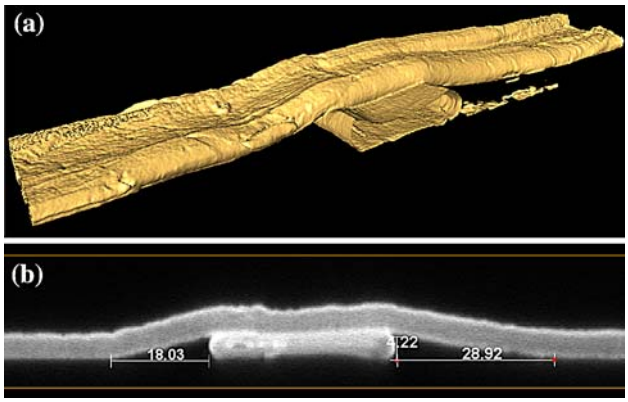

Fig. 9 CLSM 3D image of a BCTMP fiber deforms over another BCTMP fiber (**a**), and the transverse image of the fiber intersection (**b**). The sample was prepared following the same procedure as used for flexibility measurement

confirms the finding of Lowe et al. [38] with a different microscopic technique.

Based on Fig. 8, when span length is less than 30 μm, the shear contribution is over 90%. With increasing E/G ratio, shear contribution increases for the same span length. For instance, if a higher E/G ratio, 2000, is used, the shear contribution calculated is even greater. It is apparent that the shear deformation is substantial and dominating in the overall fiber deformation in a real paper structure. It can be deduced that the shear flexibility should be more effective than bending flexibility in conformability behavior of fibers during papermaking process and in paper structure. Furthermore, the area of fiber cross-section, rather than the moment of inertia, has more effect on the fiber deformation when the span is short, e.g., in the paper structure. This explains the results which are obtained by Da Silva [39],

Lossada [40], and Paavilainen [41] that the moment of inertia has little effect on paper properties.

In all hydrodynamic methods for fiber flexibility test, only long fibers have been measured and the span length subjected to the transverse are in the order of few millimeter. Therefore, the contribution of shear is less than 10% (Fig. 8) and these methods mainly measure the fiber bending flexibility. In contrast, the contribution of shear to the overall fiber deformation in the Steadman method depends on the wet press pressure used. Higher pressure results in short span length and in turn, higher shear contribution. The contribution of shear is also affected by the material properties of different types of fibers, which is characterized by their E/G ratios. By selecting the support wire of the same diameter as real fibers or using real pulp fibers as a support, fiber deformation in a real paper structure can be better simulated. The shear contributions obtained in the present study are about 60–90% for the three fiber types. Therefore, the flexibility obtained using the Steadman method is a combination of bending and shear flexibility. However, both shear and bending should be evaluated, and according to the present study, shear should be more emphasized in the analysis.

Analysis of possible errors

The method developed in this study is based on small deflection beam theory by assuming fiber as a homogeneous elastic beam, which means that fibers deform only elastically, fiber cross section is uniform, and the fiber deflection is small. In reality, fiber cross-section shape varies along fiber length and the plastic deformation can occur. Of all these factors, the deflection ratio may have the most significant influence on the measured result. The flexibility is overestimated when using small deflection beam theory to approximate the beam with large deformation, as discussed by Lawryshyn [42]. In this study, most deflection ratios are less than 25%, and the errors associated with the large deflection ratio is less than 10% according to Lawryshyn [42]. The deflection ratio can be controlled either by using small diameter glass wire or using low pressing pressure, or by using both of them. However, lower pressing pressure may decrease the binding ability of fibers to the glass slide, which may lead to spring-back problem. The ability of fibers to adhere to the glass surface is critical in this method [5]. In this experiment, it was found that it worked very well with fibers that have higher bond ability, i.e., BCTMP, refined BKP fibers, but for some rigid fibers, i.e., CTMP, the adhesion was not sufficient to hold the fibers in position when pressing load was released.

The measurement of the free span length L is also critical. The accuracy has been improved by defining a "neutral bending plane". With CLSM, fiber transverse deformation shape can be visualized, so only fibers that formed perfect bending span were measured. In fact, only for the spans of regular shape can the beam deflection theory be applied. Therefore, the accuracy and consistency of the results were also improved.

The cross-sectional dimensions of fibers are quite variable due to its nature. Although the cross-section area and the moment of inertia were measured based on each pixel on the binarized images, different locations on a fiber can give quite different results, which contributed to results scattering of the measured results.

Conclusions

A new method has been developed which can measure both bending flexibility and shear flexibility of pulp fibers based on the conformability method developed by Steadman and Luner [5]. Using CLSM, not only the shape of a fiber span over a support wire, but also the cross-section geometry of the fiber can be observed simultaneously. By developing a two-stage wet pressing process, fiber bending flexibility, shear flexibility, longitudinal elastic modulus, and shear modulus can be obtained with one test based on the beam deflection theory.

Results show that the elastic modulus of the spruce BKP fibers, aspen BCTMP fibers, and aspen CTMP fibers are about 3 GPa, 19 GPa, and 37 GPa, respectively, which is on the same order of magnitude of 10 GPa as reported in the literature. The shear modulii of the three types of pulp fibers are 28 MPa, 80 MPa, and 103 MPa, respectively, which is much larger than 5 MPa which has been suggested in the literature.

It was also found that the shear contribution to the overall fiber deformation is substantial, being about 60–90% in the present experiment setting. Shear contribution to the overall fiber deformation was also observed directly from the shape of the deformed fibers. The present results substantiate the concept of shear contribution to overall fiber deformation as proposed by Waterhouse and Page.

Acknowledgements The author would like to acknowledge the financial support of AIF, CFI, and NBIF to this research.

References

1. Forgracs OL, Robertson AA, Mason SG (1957) In: 1st fundamental research symposium, Cambridge, p 447
2. Samuelsson LG (1963) Sven Papperstidn 15(1):S41
3. Kuhn DCS, Lu X, Olson JA, Robertson AG (1995) J Pulp Pap Sci 21(1):337
4. Tam Doo PA, Kerekes RJ (1981) Tappi J 64:113
5. Steadman R, Luner P (1981) 8th fundamental research symposium, p 211

6. Waterhouse JF, Page DH (2004) Nord Pulp Pap Res J 19:89. doi:10.3183/NPPRJ-2004-19-01-p089-092
7. Mohlin UB (1975) Sven Papperstidn 78(11):412
8. Ruhlemann F (1926) Pap Trade J 82(13):T168
9. Jayne BA (1959) Tappi J 42:461
10. Leopold B (1966) Tappi J 49:315
11. Page DH, El-Hosseiny F, Winkler K (1971) Nature 229:252. doi:10.1038/229252a0
12. Ehrnrooth EML, Kolseth P (1984) Wood Fiber Sci 16(4):549
13. Page DH, El-Hossiny F, Winkler K, Lancaster APS (1970) Tappi J 60(4):114
14. Mark RE (2002) Handbook of physical testing of paper II, 2nd edn. Marcel Dekker Inc., New York
15. Mark RE (1967) Cell wall mechanics of tracheids, Yale University
16. Mcmillin CW (1974) Sven Papperstidn 77(9):319
17. Kolseth P, De R (1978) In: General constitutive relations for wood and wood-based materials, Syracuse University, pp 57–59
18. Nato T, Usuda M, Kadoya T (1983) Proc 1983 Int. Paper Physics Conf. Atlanta, TAPPI Press, Atlanta, pp 197–201
19. Faure JP, Lariviere JP, Bacon C, Pouyet J (1997) Exp Mech 37:344. doi:10.1007/BF02317429
20. Naito T, Usuda M, Kadoya T (1980) Tappi J 63:115
21. Hartler N, Nyren J (1970) Tappi J 73(5):820
22. Scallan AM, Tigerström AC (1992) J Pulp Pap Sci 18(5):J188
23. Dunford JA, Wild PM (2002) J Pulp Pap Sci 28:136
24. Chhabra N, Spelt JK, Yip CM, Kortschot MT (2005) J Pulp Pap Sci 31:52
25. Scallan AM, Tigerstrom AC (1992) J Pulp Pap Sci 18:188
26. Yan D, Li K (2007) J Mater Sci. doi:10.1007/s10853-007-2085-9
27. Yan D, Li K, Zhou Y (2008) Tappi J 91:25
28. Ebeling K (1976) In: Bolam F (ed) Technical division. BPBIF, London, pp 304–335
29. Nesbakk T, Helle T (2002) Proceeding of 88th annual meeting of pulp and paper technical association of Canada, p 113
30. Gao Y, Li K, Wang Z (2007) Pulp Pap Can 108(1):44
31. Gere JM, Timoshenko SP (1990) Mechanics of materials, PWS-KENT, USA
32. Abramoff MD, Magelhaes PJ, Ram SJ (2004) Biophotonics Int 11(7):36
33. Harlick RM, Linda GS (1992) Computer and robot vision. Addison-Wesley
34. Li K, Tan X, Yan D (2006) Surf Interface Anal 38(1):1328. doi:10.1002/sia.2454
35. Cousins WJ (1976) Wood Fiber Sci 10:9
36. Nyren J (1971) Pulp Pap Can 72(10):T321
37. Wild P, Omholt I, Steinke D, Schuetze A (2005) J Pulp Pap Sci 31:116
38. Lowe R, Ragauskas A, Page DH (2005) In: I'Anson SJ (ed) Advances in paper science and technology, Proc 13th fundamental research symposium, FRC Manchester, p 921
39. Da Silva EC (1983) In: Tappi proceedings 1983 International paper physics conference, p 13
40. Lossada AA (1998) Paperi ja Puu 80:257
41. Paavilainen L (1993) Paperi ja Puu 75(9):689
42. Lawryshyn YA, Kuhn DCS (1996) J Pulp Pap Sci 22(1):423